Airborne EM MobileMTm – technical details and applications

Aamna Sirohey, Expert Geophysics Limited*
Alexander Prikhodko, Expert Geophysics Limited
Andrei Bagrianski, Expert Geophysics Limited
Petr Kuzmin, Expert Geophysics Limited

Summary

The MobileMTm airborne electromagnetic system, designed by Expert Geophysics Limited, is a modified version of the original MobileMT system. The modified system utilizes naturally occurring EM fields over a broad frequency range (90 – 27,000 Hz) to recover the conductivity structure over a wide range of depths and is outfitted with two magnetic sensors configured to measure the horizontal gradient of the magnetic field. The modifications made to the original design are geared toward better identification and imaging of discrete targets and complex structures in the depth range from the surface to several hundreds of meters for both electromagnetic and magnetic datasets. To test the capabilities of the modified system, two test blocks were flown over two known kimberlite pipes in the Lake Timiskaming kimberlite field of northeastern Ontario (KL-01 & KL-22). The output apparent conductivity and horizontal gradient magnetic data from the MobileMTm system, clearly delineate the locations of the kimberlites. 1-D and 3-D inversion results illustrate conductivity structure to depths of 700 m and elucidate the 'pipe-like' structure of the kimberlites at depth. This case study demonstrates the ability of MobileMTm to aid in the identification of discrete targets, such as kimberlites, located at the surface/near-surface and ranging up to several hundreds of meters depth.

Introduction

EGL's proprietary MobileMT (Mobile Magnetotellurics) technology utilizes the Earth's naturally occurring, or passive, electromagnetic (EM) fields to image the earth's subsurface conductivity structure. The use of naturally occurring EM fields as a source of 'transmitted' energy, overcomes many limitations inherent to other airborne EM systems and principles. The main advantages of using passive EM fields are that the depth of investigation always exceeds the capabilities of systems with controlled sources; the method is not only sensitive to conductors, but also resistivity differences in the range of thousands of ohm-m's; and there is no critical dependence on terrain clearance/flying height.

From a theoretical point of view, the original MobileMT system and MobileMTm relate to the same principle and function identically. However, modifications to the airborne component render the modified system better suited to identify discrete, near surface targets. Where the MobileMT airborne EM component is towed using a 96 m tow cable, with a separate magnetometer located 20 m above the EM sensor, the airborne component of the MobileMTm technology is towed using a 55 m tow cable, and the EM sensor, as well as two magnetometers, configured to measure the horizontal gradient of the magnetic field, are located on the same frame (Figure 1). In addition, the airborne bird for the MobileMTm system is equipped with a GPS antenna and a gyro inclinometer on the frame, allowing accurate retrieval of positions for both the airborne EM sensor, and magnetometers.

Figure 1. Airborne component of original MobileMT (top), and modified MobileMTm (bottom) systems.

Theory

The MobileMT technology consists of a stationary ground base station, which measures main, and reference electrical signals intended to provide bias-free and denoised orthogonal, horizontal component electric field data, as well as a towed airborne receiver for measurement of variations in the three magnetic components of naturally occurring EM fields. The variations of the EM field are measured in the frequency range from 26 Hz to 27 kHz (90 Hz-27 kHz for MobileMTm), then digitized and recorded at 74 kHz to produce a representative time series dataset (Figure 2).

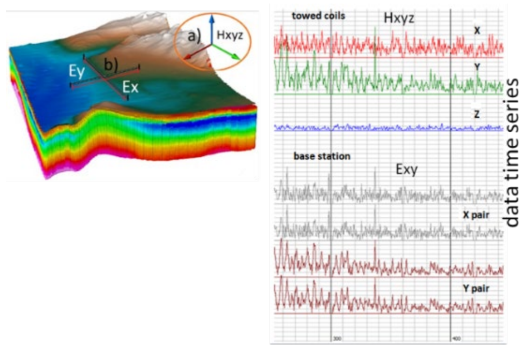

Figure 2. MobileMT Technology.

Fast Fourier techniques are applied to the merged time series data to calculate six admittance matrices for different time windows and in different frequency bands. Modular computation of the matrices' determinants, which are rotation invariant parameters, result in apparent conductivity calculated for ~30 frequency windows as the main output parameter of MobileMT mapping (Figure 3).

H towed coils   ***E*** base station

$$H = \begin{bmatrix} Hx \\ Hy \\ Hz \end{bmatrix} \qquad E = \begin{bmatrix} Ex \\ Ey \\ 0 \end{bmatrix}$$

$$\begin{bmatrix} Hx \\ Hy \\ Hz \end{bmatrix} = \begin{bmatrix} Yxx & Yxy \\ Yyx & Yyy \\ Yzx & Yzy \end{bmatrix} \begin{bmatrix} Ex \\ Ey \end{bmatrix}$$

$$\sigma = \mu\omega|Y^2|$$

Figure 3. Computation of apparent conductivity from MobileMT H and E-field data.

Kimberlite exploration in Ontario

Worldwide, most diamond deposits are hosted in kimberlite rock. Kimberlites are magmatic rocks that form deep in Earth's interior and are brought to the surface through eruptive processes. As they are erupted toward the surface, the magmas may assimilate other types of minerals, referred to as xenoliths. If they originate at, or below, the "diamond stability field", they can bring diamonds to the surface (Kennedy & Kennedy, 1976).

Kimberlites in north-eastern Ontario occur along a trend oriented at ~325°, which the Lake Timiskaming Structural Zone is one expression. Many kimberlites of the Lake Timiskaming Structural Zone occur at intersections between the regional northwesterly trend, and local lineaments, faults, and lithologic boundaries (Sage, 2000). The bedrock geology mainly consists of Paleoproterozoic Huronian Supergroup rocks, and later intrusive Nippising Diabase dykes and sills. Glacial and lacustrine deposits variably mantle bedrock (Sobie, 2004).

Geophysical responses over kimberlite pipes are complex due to inhomogeneity of the internal properties of kimberlites, as well as the host rock in which they have been emplaced (see Macnae, 1979). Kimberlite generally contains ~5 to 10% iron in the form of oxides, and in the unweathered material, some of this is often present as magnetite (Fesq et al., 1975). Aeromagnetic data are thus widely used to locate kimberlite pipes. However, kimberlites can produce positive, negative, as well as no magnetic anomaly, depending on the degree of weathering, contrast between the magnetic properties of the kimberlite and the host rock, and remnant magnetization.

In the absence of a clear magnetic signature, airborne EM data have proven to be useful. Conductive anomalies often develop in crater facies kimberlite because of weathering of ultra-basic kimberlite minerals (Palacky, 1986), as well as due to high porosity in tuffaceous and brecciated parts of the pipe (diatreme facies) that may act as a conduit for groundwater flow (Macnae, 1995). This means that a kimberlite may produce a conductive anomaly that will extend from the crater facies (surface) to the diatreme facies (at depth), depending on the overburden electrical properties and thickness, and the electrical properties of the host rock.

Other challenges for kimberlite exploration with geophysical methods include possible small dimensions of pipes, which can be as small as 75 m in diameter (Kjarsgaard, 2007), and the parasitic induced polarization effect corrupting transient EM (time-domain) data (Kwan et al., 2015). Therefore, when evaluating the utility of geophysical techniques to prospect for kimberlites, variable responses and the ultimate effectiveness of the method should be considered.

MobileMTm field data over Kimberlite Pipes

A MobileMTm survey was conducted in July 2021 over two known kimberlite pipes located in north-eastern Ontario (Kl-01 & KL-22), in the west part of the Lake Timiskaming kimberlite field (Figure 4).

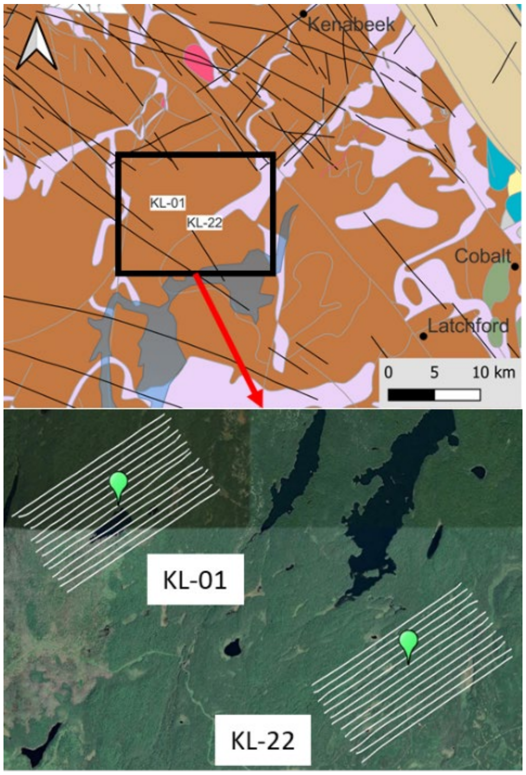

Figure 4. Location of MobileMTm survey areas over two known kimberlite pipes. Bedrock geology map from https://www.geologyontario.mndm.gov.on.ca/ogsearth.html.

The KL-01 and KL-22 kimberlites were discovered in the Klock and van Nostrand townships in 2004 by Contact Diamond Corp. using a combination of till sampling and geophysical methods (Sobie, 2004). From the results of drilling, the KL-01 kimberlite is known to be covered by approximately 14 m of glacial overburden and is deeply weathered. The KL-22 kimberlite is covered by more than 30 m of glacial sediments and is fresh at its subcropping surface (McClenaghan et al., 2008). The bedrock geology in the vicinity of the kimberlites consists of Paleoproterozoic rocks of the Lorrain and Gowganda formation. Both kimberlites follow an azimuth parallel to the Kerry Lake fault (325°) and have an elongated morphology following this trend; KL-01 (~150 m x 300 m), KL-22 (~140 m x 420 m) (McClenaghan et al., 2008). Both kimberlites are known to form positive magnetic anomalies as they dominantly consist of volcaniclastic kimberlite, with some late-stage cross-cutting hypabyssal kimberlite (Sobie and Long, 2006).

Two ~3.25 km^2 blocks were flown over the two kimberlites. Lines were flown at a 100 m spacing and azimuth of 55° (NE). The MobileMTm survey data recorded by the towed bird sensor (three mutually orthogonal dB/dt components of the EM field) were merged with the two mutually orthogonal components of the electric field from the stationary base station, and apparent conductivities were calculated for different frequency bands. Select frequencies were extracted for data processing based on signal strength. The processed apparent conductivity data were then inverted using a 1-D non-linear least squares iterative inversion routine developed by N. Golubev for the MobileMT technology to derive resistivity-depth distributions for each measurement station. The inversion algorithm is based on the conjugate gradient method with adaptive regularization (Zhdanov, 2002). The MobileMTm data were also inverted by Geotexera Inc. using a 3-D inversion software developed by Dr. Colin Farquharson's research group at the Memorial University of Newfoundland (Jahandari & Farquharson, 2017).

Results

The MobileMTm data acquired over the KL-01 kimberlite block clearly demonstrate a conductive anomaly on a series of frequencies (from 102 to 17099 Hz), centered on the location of the known kimberlite, which is coincident with a magnetic high (Figure 5).

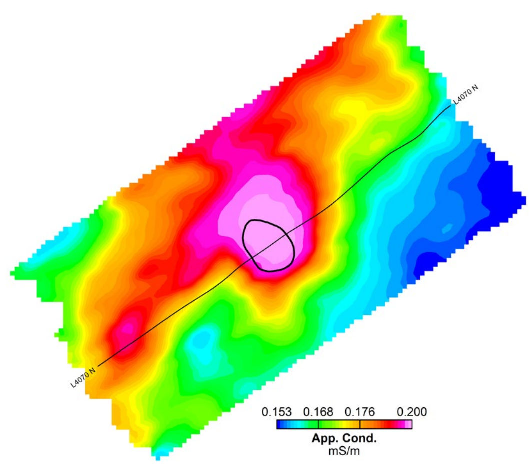

Figure 5. Map of apparent conductivity at 8550 Hz, with main magnetic contour (54990 nT) overlain.

The location of the kimberlite is clearly evidenced by the apparent conductivity profile data (Figure 6). Vertical cross-sections showing the inverted resistivity-depth distribution image the extent of the anomaly source in 2-D (Figure 7). Both the results of 1-D and 3-D inversion show a similar picture in terms of the extent of the kimberlite, both at the surface and with depth.

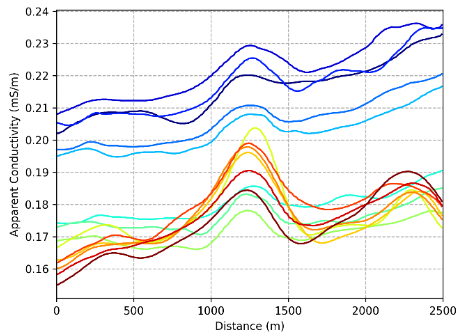

Figure 6. Apparent conductivity profile data for several frequencies along L4070 (shown in plan view in Figure 5). Cooler color profiles correspond to lower frequencies and warmer color profiles correspond to higher frequencies.

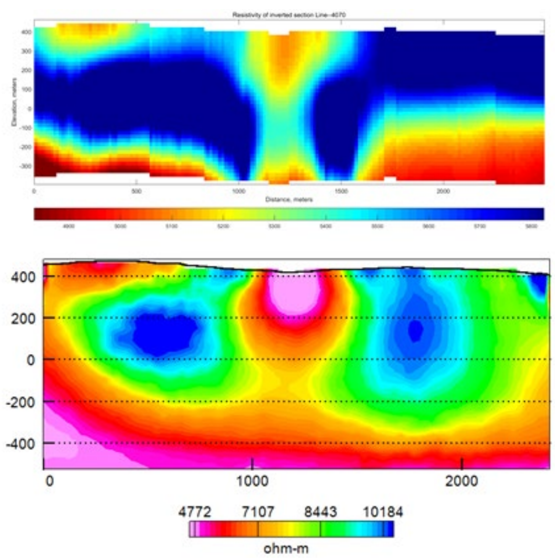

Figure 7. Vertical cross sections showing resistivity-depth model calculated from 1-D inversions (top), and 3-D inversions (bottom).

The pipe-like structure of the kimberlite in 3-D can be visualized by isolating the conductive volumes of the 3-D resistivity model (Figure 8). The drilling results summarized in Sobie (2004) indicate that the KL-01 kimberlite consists of "matrix-supported magmaclastic macrocrystic kimberlite with a segregationary inter-clast matrix" from 13.7 to 35.8 m depth, and then from 35.8 to 156.4 m depth, "matrix supported magmaclastic macrocrystic kimberlite breccia with non-magmatic interclast matrix", which is common for diatreme facies, and may explain the presence of the conductive anomaly.

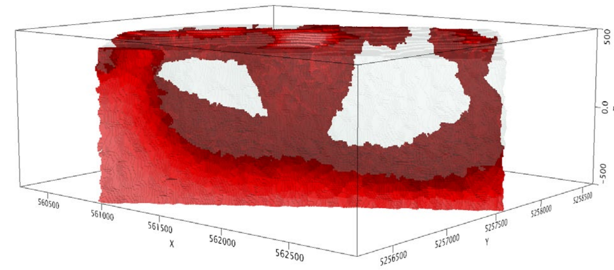

Figure 8. Conductive volumes from resistivity-depth model derived from 3-D inversions, clearly demonstrating the pipe-like structure of the kimberlite.

Similar results were obtained for the KL-22 kimberlite block (Figure 9).

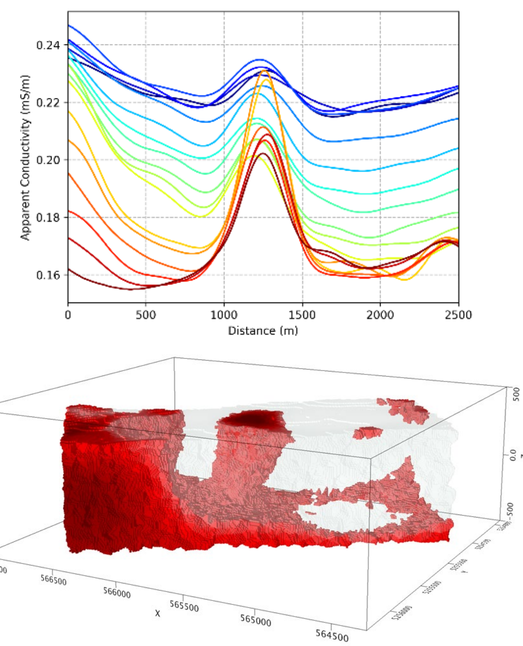

Figure 9. Apparent conductivity profiles for line that transects KL-22 kimberlite (top). Conductive volumes of resistivity-depth model derived from 3-D inversions (bottom).

The ability of the MobileMTm airborne bird component to simultaneously measure the horizontal gradient of the magnetic field has several advantages including improved resolution of shallow features and closely spaced sources, and easier detection of pipe-like sources when compared to non-gradient magnetic methods, which are advantageous for applications such as kimberlite exploration (Schmidt & Clark, 2000). The location of the kimberlite can be seen clearly in both the total field and horizontal gradient data (Figure 10).

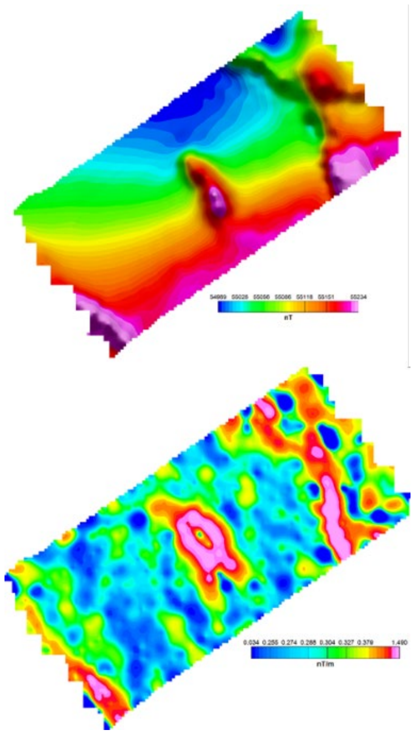

Figure 10. Map of total magnetic field for KL-22 block (top), map of horizonal gradient of magnetic field (bottom).

Conclusions

This case study demonstrates the potential of the MobileMTm system to aid in the identification of discrete targets including kimberlites, located in the near surface, and ranging up to several hundreds of meters depth, through acquisition of magnetic and electromagnetic data. The output apparent conductivities of the MobileMTm system for the test blocks, particularly at higher frequencies, clearly delineate the locations of the kimberlite. Inversion results illustrate conductivity structure to depths of 700 m and elucidate the 'pipe-like' shape of the kimberlites at depth. In addition to the greater depth of investigation, the passive field technology can detect superconductors and distinguish between rock types with high resistivities, i.e., in excess of thousands and tens of thousands of ohm-m, and is free of distortions from parasitic induced polarization and super-paramagnetic effects inherent to systems with impulse type, artificially driven transmitters. This makes the technology suitable for use in a range of geological environments, terrain conditions and for varied exploration applications.

References

Fesq, H. W., Kable, E. J. D., & Gurney, J. J. (1975). Aspects of the geochemistry of kimberlites from the Premier mine, and other selected South African occurrences with particular reference to the rare earth elements. In Physics and Chemistry of the Earth (pp. 687-707). Pergamon.

Jahandari, H., & Farquharson, C. (2017). 3-D minimum-structure inversion of magnetotelluric data using the finite-element method and tetrahedral grids, Geophysical Journal International, 211, 1211-1227.

Kennedy, C. S., & Kennedy, G. C. (1976). The equilibrium boundary between graphite and diamond. Journal of Geophysical Research, 81(14), 2467-2470.

Kjarsgaard, B. A. (2007). Kimberlite pipe models: significance for exploration. In Proceedings of exploration (Vol. 7, pp. 667-677).

Kwan, K., Prikhodko, A., Legault, J. M., & Goncharov, E. (2015, October). Airborne inductively induced polarization effects in and their removal from the VTEM data from Mirny, Russia. In 2015 SEG Annual Meeting.

Macnae, J. C. (1979). Kimberlites and exploration geophysics. Geophysics, 44(8), 1395-1416.

Macnae, J. (1995). Applications of geophysics for the detection and exploration of kimberlites and lamproites. Journal of Geochemical Exploration, 53(1-3), 213-243.

McClenaghan, M.B., Kjarsgaard, I.M., and Kjarsgaard, B.A. (2008). Indicator Mineral Chemistry of the KL-01 and KL-02 Kimberlites, Lake Timiskaming Kimberlite Field, Ontario; Geological Survey of Canada, Open File 5800, 1 CD-ROM.

McIlwaine, W.H. and Card, K.D. (1973). Geology, Makobe Lake; Ontario Geological Survey, Map 2257, scale 1:63,360.

Palacky, G. J. (1986). Airborne Resistivity Mapping. Geological Survey of Canada, Paper 86-22.

Sage, R.P. (2000). Kimberlites of the Lake Timiskaming structural zone: supplement; Ontario Geological Survey, Open File Report 6018, 123p.

Schmidt, P. W., & Clark, D. A. (2000). Advantages of measuring the magnetic gradient tensor. Preview, 85, 26-30.

Sobie, P. (2004, June 07). Report on 2003-2004 exploration on the Klock Property Larder Lake mining division, northeastern Ontario of Sudbury Contact Mines Limited.

Sobie, P. and Long, G. (2006). Technical report on the Timiskaming diamond project, NE Ontario and NW Quebec of Contact Diamond Corporation. Digital company report on SEDAR website http://www.sedar.com.

Zhdanov, M. (2002). Geophysical Inverse Theory and Regularization Problems Methods in Geochemistry and Geophysics, 36. Elsevier, 609 p.